Submitted, Physical Review Letters, 2008
http://www.cds.caltech.edu/~murray/papers/2008u_om08-prl.html

Dynamics, Geometry, and Stability of Low Reynolds Number Swimming Near a Wall

Yizhar Or* and Richard M. Murray
Dept. of Control and Dynamical Systems, California Institute of Technology, 1200E California Blvd., Pasadena, CA 91125, USA
(Dated: November 18, 2008)

We study the dynamics of low Reynolds number swimming near a plane wall by using a simple theoretical swimmer model that accounts for far-field hydrodynamic interactions. We focus on steady motion parallel to the wall and derive conditions under which it is *passively stable without sensing or feedback*. We highlight the geometric structure of the swimming equation and particularly the relation between stability and *reversing symmetry* of the wall-swimmer dynamics. Furthermore, in the case of unstable parallel swimming, our numerical simulations reveal the existence of a *stable periodic motion* along the wall, associated with a degenerate Hopf bifurcation.

PACS numbers: 47.63.mf, 45.80.+r, 47.10.Fg

Introduction: The swimming of microorganisms, as well as of tiny robotic swimmers, is governed by low Reynolds number (*Re*) hydrodynamics, where viscous effects dominate and inertial effects are negligible [1–3]. The study of low-*Re* swimming has recently gained increasing interest, mainly for investigating the behavior of swimming microorganisms and motile cells, and for laying basic theoretical foundations towards development of micron-scale artificial swimmers for performing in-body biomedical tasks. Many works have analyzed the dynamics of swimming in *unbounded fluid* by exploiting its geometric structure, namely the *gauge symmetry* [4–6], while some recent works study this problem in the context of control theory [7, 8]. However, in reality, swimmers often move in a confined environment, where their hydrodynamic interactions with the boundary is complicated to model [9, 10]. Moreover, breaking the gauge symmetry raises problems such as steering to a desired direction and dynamic stability of the motion under perturbations.

In this paper, we analyze the dynamics and stability of low-*Re* swimming near a plane wall. Unlike classical models such as [11, 12] that utilize shape changes to induce self-propulsion, we focus on a special subclass of swimmers, having an *apparently constant shape*, reminiscent of vehicles that move by rotating their wheels or tracks. Examples of such swimmers are the twirling torus [13] and the surface treadmiller [14], inspired by actin-based cell motility [15]. Focusing on a model of swimmer propelled by rotating spheres, we formulate the swimming equation by utilizing the hydrodynamic model in [16]. We study the underlying geometric structure of the dynamics, and show that it is associated with a *reversing symmetry* [17] of the wall-swimmer configuration. We analyze swimming motion parallel to the wall, and derive conditions under which it is *passively stable* under perturbations. In particular, we show that one has to break the reversing symmetry in order to obtain asymptotic stability. The implication of passive stability in the context of artificial swimmers is that they can be steered by open-loop commands only, without requiring on-board sensing and control for stabilization. In biological systems, this result may serve as a key in explaining phenomena such as accumulation of swimming microorganisms and motile cells near boundaries [18, 19]. Finally, in the case of unstable parallel swimming, we present numerical simulations that reveal the existence of a *stable periodic motion* along the wall, which is associated with a degenerate Hopf bifurcation [20].

Kinematic model: We consider a simple model of a micro-swimmer comprised of n rigid spheres of equal radius a, which are connected by a thin rigid frame, called the *body* of the swimmer. The swimmer is submerged in a viscous fluid which is bounded by an infinite plane wall at $y = 0$ [Fig. 1]. The spheres and the rigid frame all lie within the xy plane, and all motions are assumed to be constrained to that plane. The spheres labeled $1 \dots m$ are actuated by rotation about their z-axis which is attached to the frame, while the rest of the spheres are rigidly attached to the frame. Let $\mathcal{F}_w$ be a world-fixed reference frame, and let $\mathcal{F}_b$ be a reference frame attached to the swimmer's body. Let $u_i \in I\!R$, be the angular velocity of the ith sphere with respect to the body, and denote $\mathbf{u} = (u_1 \dots u_m)^T$, which is regarded as the swimmer's input. Let $\mathbf{q} = (x, y, \theta)^T \in SE(2)$ denote the position and orientation of the body expressed in the world frame $\mathcal{F}_w$. Let $\mathbf{r}_i$ be the constant position vector of the ith sphere expressed in the body frame $\mathcal{F}_b$. Let $\mathbf{V}_i \in I\!R^2$ denote the linear velocity of the ith sphere in xy plane, and let $\omega_i \in I\!R$ be its angular velocity about the z axis. The linear velocity of the ith sphere satisfies $\mathbf{V}_i = (\dot{x}\ \dot{y})^T + \mathbf{D}(\theta)\mathbf{r}_i\dot{\theta}$, where $\mathbf{D}(\theta) = \begin{pmatrix} -\sin\theta & -\cos\theta \\ \cos\theta & -\sin\theta \end{pmatrix}$. The angular velocity of the ith sphere is given by $\omega_i = \dot{\theta} + u_i$ for $i = 1 \dots m$, and $\omega_i = \dot{\theta}$ for $i = m+1 \dots n$. Defining $\mathbf{U} = (\mathbf{V}_1, \dots \mathbf{V}_n, \omega_1, \dots, \omega_n)^T$, the velocity relations above can be written in matrix form as $\mathbf{U} = \mathbf{T}\dot{\mathbf{q}} + \mathbf{E}\mathbf{u}$.

Hydrodynamic forces: We now derive expressions for the hydrodynamic forces and torques acting on each sphere and on the swimmer's body, assuming that the hydrodynamic resistance of the thin body

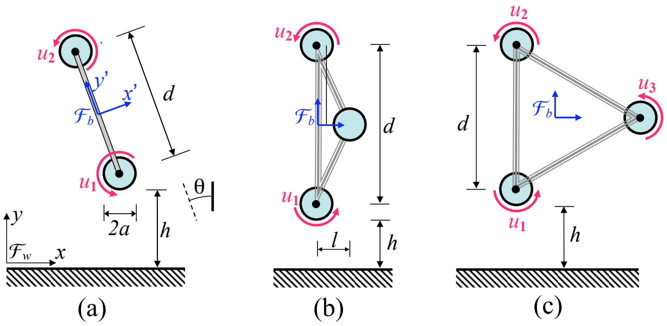

FIG. 1: Drawing of the swimmers- (a): Two-sphere swimmer. (b): 2+1 sphere swimmer. (c): Three-sphere swimmer.

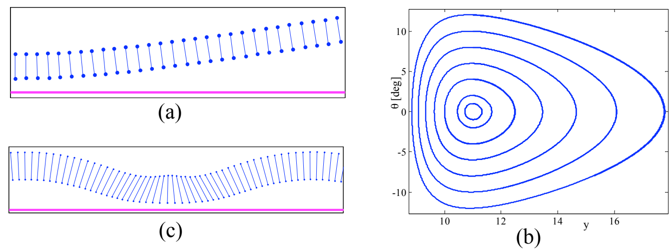

FIG. 2: The two-sphere swimmer - (a): Snapshots of the motion for $u_1 = -u_2$. (b): Phase plot in (y, θ) plane for a marginally stable equilibrium $\mathbf{q}_e'$. (c): Snapshots of periodic motion along the wall.

frame is negligible compared to that of the spheres. Let $\mathbf{f}_i$ and τ_i be the force and torque (about the z axis) exerted by the fluid upon the ith sphere, and define $\mathbf{F} = (\mathbf{f}_1, \ldots \mathbf{f}_n, \tau_1, \ldots, \tau_n)^T$. Let $\mathbf{F}_b = (\mathbf{f}_b, \tau_b)^T$ denote the net force and torque acting on the body. It is then straightforward to show that $\mathbf{F}_b$ satisfies $\mathbf{F}_b = \mathbf{T}^T\mathbf{F}$. The linearity of Stokes equations implies the existence of a linear relation between hydrodynamic forces and velocities, given by $\mathbf{F} = \mathbf{RU}$, where $\mathbf{R}$ is called the *resistance matrix*, and depends only on the configuration of the particles [1]. Generally, $\mathbf{R}$ cannot be computed exactly, except for simple geometries such as a single spheroid or two spheres in unbounded fluid [2]. However, in many cases $\mathbf{R}$ can be approximated by using scaling arguments. In this work, we adopt the far-field hydrodynamic model by Swan and Brady [16], which computes the *mobility matrix* defined as $\mathbf{M} = \mathbf{R}^{-1}$, for multiple spherical particles in the presence of a plane wall, assuming that all particle-particle and particle-wall separation distances are much larger the spheres' radii.

Equation of swimming: Using all the relations above, the requirement that the swimmer's body is force- and torque-free at all times, $\mathbf{F}_b = 0$ gives $\mathbf{T}^T\mathbf{R}(\mathbf{T}\dot{\mathbf{q}} + \mathbf{Eu}) = 0$. Inverting this equation gives the *swimming equation*, which formulates the relation between the input velocities and the body velocity as

$$\dot{\mathbf{q}} = \mathbf{G}(\mathbf{q})\mathbf{u}, \quad \text{where } \mathbf{G}(\mathbf{q}) = (\mathbf{T}^T\mathbf{R}\mathbf{T})^{-1}\mathbf{T}^T\mathbf{R}\mathbf{E}. \quad (1)$$

Note that in unbounded fluid, the swimmer's motion is invariant under rigid body transformations (cf. [4, 21]), which implies the following simplification. Let $\mathbf{U}_{body} = (\mathbf{V}_{body}, \omega_{body})^T$ denote the velocity of the body expressed in the body frame $\mathcal{F}_b$. The swimming equation (1) then takes the form $\mathbf{U}_{body} = \mathbf{Gu}$, where the constant matrix $\mathbf{G}$ is obtained by evaluating $\mathbf{G}(\mathbf{q})$ at a configuration where the two frames $\mathcal{F}_w$ and $\mathcal{F}_b$ are parallel. Obviously, this simplification does not hold in bounded fluid domains.

The two-sphere swimmer: Consider a simple swimmer which consists of two actuated spheres (i.e. $m = n = 2$), connected by a thin rigid rod, where the center-center separation between the spheres is denoted d [Fig. 1(a)]. In the rest of this paper, we normalize all lengths by the radius a, and set $a = 1$. The 3×2 matrix $\mathbf{G}(\mathbf{q})$ for this swimmer is derived according to (1), where the mobility matrix $\mathbf{M}$ is computed by using the model in [16]. The analytical expressions in the components of $\mathbf{G}(\mathbf{q})$ are too lengthy to be detailed here, and numerical values were computed throughout this work by using MATLAB. Note that in unbounded fluid, equal and opposite input velocities $u_1 = -u_2$ result in swimming in a straight line along the x' axis, similar to the result in [13] for the axisymmetric twirling torus. However, the presence of wall breaks the axisymmetry of the swimmer, and for $u_1 = -u_2$ it is repelled from the wall and swims along an arc, as shown in the snapshots in Fig. 2(a). Therefore, we consider the simplest task for this swimmer — steady motion parallel to the wall, i.e. in the x direction, with fixed orientation and fixed distance from the wall. As a preliminary step, we analyze the underlying geometric structure of the dynamics. A first observation is that the motion is invariant under shifting parallel to the wall in the x direction. Therefore, $\mathbf{G}(\mathbf{q})$ depends only on the coordinates y and θ, and not on x. The second observation is that the two-sphere swimmer possesses a *mirror symmetry* about the line perpendicular to the wall, which can be formulated as

$$\mathbf{G}(\mathbf{Sq}) = -\mathbf{S}\mathbf{G}(\mathbf{q}), \text{ where } \mathbf{S} = \mathsf{diag}(-1, 1, -1). \quad (2)$$

The physical meaning of (2) is that a mirror-reflected swimmer will swim along a reflected trajectory with its input velocities $\mathbf{u}$ reversed, which is equivalent to reversing the time. Formally, a relation of the form (2) is called a *reversing symmetry* of a dynamical system (cf. [17]). The reversing symmetry (2) dictates constraints on the elements of $\mathbf{G}(\mathbf{q})$ and their derivatives at the perpendicular orientation $\theta = 0$, as follows:

$$G_{2j}(\theta = 0) = 0 \quad (3)$$

$$\frac{\partial}{\partial y} G_{2j}\Big|_{\theta=0} = 0 \, , \; \frac{\partial}{\partial \theta} G_{3j}\Big|_{\theta=0} = 0 \quad (4)$$

for $j = 1, 2$, where G_{ij} is the (i, j) element of $\mathbf{G}(\mathbf{q})$. The constraint (3) implies that when $\theta=0$, the $\dot{y}$-component of $\dot{\mathbf{q}}$ vanishes for any y and $\mathbf{u}$. Therefore, for any given distance from the wall $y=y_e$, taking constant input velocities $\mathbf{u}_e=\alpha(-G_{32},G_{31})$ where G_{31},G_{32} are evaluated at $(y,\theta)=(y_e,0)$ and $\alpha\in I\!R$, the $\dot{\theta}$- component of $\dot{\mathbf{q}}$ also vanishes, resulting in swimming velocity of the form $\dot{\mathbf{q}}=(v_x,0,0)$, which corresponds to steady swimming parallel to the wall with $\theta=0$.

Next, we analyze the *dynamic stability* of parallel swimming. Denoting $\mathbf{q}'=(y,\theta)$, the dynamics of $\mathbf{q}'$ is given by

$$\dot{\mathbf{q}}'=\mathbf{G}'(\mathbf{q}')\mathbf{u} \qquad (5)$$

where $\mathbf{G}'$ is the lower 2×2 block of $\mathbf{G}(\mathbf{q})$ in (1). By construction, the system (5) has an equilibrium point at $\mathbf{q}'_e=(y_e,0)$ under the constant input $\mathbf{u}=\mathbf{u}_e$. Formally, $\mathbf{q}'_e$ is called a *relative equilibrium* of (1) [22]. The local stability of $\mathbf{q}'_e$ is determined by the *linearization* of (5) about $\mathbf{q}'_e$, given by

$$\delta\dot{\mathbf{q}}'=\mathbf{A}\delta\mathbf{q}',\text{ where }\mathbf{A}=\left.\frac{\partial\mathbf{G}'(\mathbf{q}')}{\partial\mathbf{q}'}\right|_{\mathbf{q}'_e}\cdot\mathbf{u}_e. \qquad (6)$$

A sufficient condition for asymptotic stability of $\mathbf{q}'_e$ is that all eigenvalues of $\mathbf{A}$ have negative real part. However, invoking the constraints (4), the linearization matrix $\mathbf{A}$ takes the form $\mathbf{A}=\begin{pmatrix}0 & b\\ c & 0\end{pmatrix}$, and its characteristic polynomial is $\Delta_A(\lambda)=\lambda^2-bc$. Note that the eigenvalues are a symmetric pair $\pm\lambda$, typical for reversible systems where existence of a solution behaving like $e^{\lambda t}$ implies the existence of a reflected time-reversed solution behaving like $e^{-\lambda t}$. The real part of the eigenvalues depends on the sign of bc, as follows. If $bc>0$, $\mathbf{A}$ has two real eigenvalues of the form $\lambda=\pm\sqrt{bc}$, and $\mathbf{q}'_e$ is *unstable*. If $bc<0$, $\mathbf{A}$ has a pair of imaginary eigenvalues $\lambda_{1,2}=\pm i\sqrt{|bc|}$. Moreover, the reversing symmetry implies that $\mathbf{q}'_e$ is a *reversible Lyapunov center* [17, 23], which is a marginally stable equilibrium point enclosed by a one-parameter family of periodic orbits. In order to determine the sign of bc, we explicitly formulate the Jacobian matrix $\mathbf{A}$, by applying the chain rule to the definition of $\mathbf{G}(\mathbf{q})$ in (1) and differentiating the elements of $\mathbf{M}$ in [16] with respect to y and θ. Using this procedure, we numerically compute the product bc as a function of h, where $h=y-a-0.5d\cos\theta$ [Fig. 1(a)], for different values of d. The results, which are plotted in Fig. 3(a), show that when the wall-separation h is sufficiently large, bc is negative, and $\mathbf{q}'_e$ is a marginally stable equilibrium. Fig. 2(b) shows the phase portrait in (y,θ) plane for $d=10$ under constant input $\mathbf{u}_e=(1,-1.0017)$ associated with $\mathbf{q}'_e=(11,0)$. Fig. 2(c) depicts snapshots of the periodic motion along the wall for a specific (y,θ)-trajectory.

Next, since swimming in perpendicular orientation cannot be asymptotically stable, we seek for steady parallel swimming at *asymmetric orientations* of the swimmer, i.e. try to find equilibrium points of (5) for $\theta\neq 0$. A necessary condition for equilibrium is that the columns of the matrix $\mathbf{G}'(\mathbf{q}')$ are linearly dependent, so that $\mathbf{G}'(\mathbf{q}')\mathbf{u}=0$ for some input $\mathbf{u}$. In the following, we numerically compute $\det\mathbf{G}'$ as a function of θ when h is held constant. The results are shown in Fig. 3(b) for $h=5$ (thick blue) and $h=2$ (thin red). For large separations such as $h=5$ and above, the only zero-crossing is at $\theta=0$, corresponding to the perpendicular orientation. However, for the smaller separation $h=2$, there exists an additional zero-crossing point at $\theta=61.25°$, with corresponding input vector $\mathbf{u}_e=(1,-1.017)^T$. Numerical computation of the linearization matrix $\mathbf{A}$ and its eigenvalues gives $\lambda_1=-0.0012$, $\lambda_2=0.0008$, hence the equilibrium point $\mathbf{q}'_e$ is *unstable.* Similar results were obtained numerically for other values of d and h.

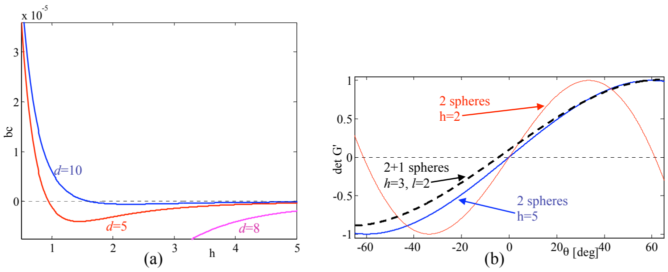

FIG. 3: (a): Plot of bc as a function of h for the two-sphere swimmer with $\theta=0$. (b): Plot of $\det G'(\theta)$ for the two-sphere swimmer with $h=5$ (thick blue) and $h=2$ (thin red), and for the 2+1-sphere swimmer with $h=3,\ l=2$ (dashed black).

The 2+1-sphere swimmer: The next step is breaking the symmetry by *changing the structure* of the swimmer. This is done by adding an additional unactuated sphere which is rigidly attached to the swimmer's body and forms an isosceles triangle with the two actuated spheres, having height l [Fig. 1(b)]. The condition for existence of steady parallel swimming is again $\det\mathbf{G}'=0$. As an example, $\det\mathbf{G}'$ as a function of θ for $d=10$, $l=2$, and $h=3$ is shown in Fig. 3(b) (dashed black). Due to the symmetry breaking, the zero crossing point is slightly shifted from $\theta=0$, giving an equilibrium point $\mathbf{q}'_e=(8.9866,-4.19°)$ under the input $\mathbf{u}_e=(-1,1.0086)$. Computing the eigenvalues of the associated linearization matrix $\mathbf{A}$ gives $\lambda_{1,2}=(-0.3984\pm 1.5341i)\cdot 10^{-3}$, which implies that the steady swimming is *asymptotically stable*. Fig. 4(a)-(b) show simulation results of $y(t)$ and $\theta(t)$ for this swimmer with constant input $\mathbf{u}=\mathbf{u}_e$, under initial perturbation of $\mathbf{q}'(0)=\mathbf{q}'_e+(10,20°)$. Fig. 4(c) shows snapshots of the swimmer's motion along the wall. It is clearly seen that the swimmer is passively stabilized at $\mathbf{q}'_e$ without applying any feedback.

Note that the stability result does not depend on the details of a specific hydrodynamic model. The only requirement in order to guarantee asymptotic stability for some $l\neq 0$ is that the reflection-symmetric equilibrium configuration with $l=0$ (i.e. the three spheres lie along

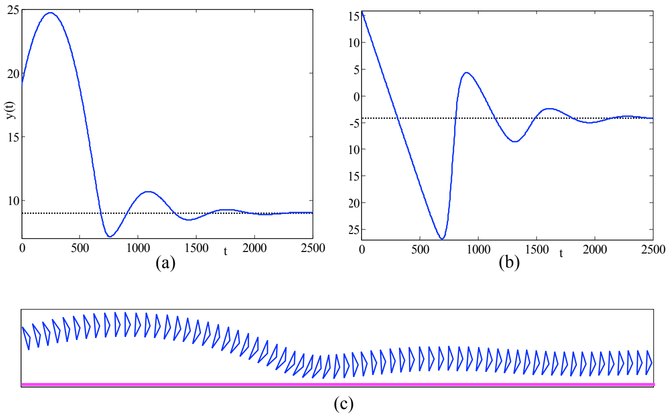

FIG. 4: Simulation of the $2+1$-sphere swimmer - (a): Plot of $y(t)$ (b): Plot of $\theta(t)$. (c): Snapshots of the swimmer's motion along the wall

a line) is marginally stable and satisfies $bc < 0$, as explained above. Under this requirement, small changes in l will cause continuous change of the eigenvalues, resulting in their movement to either the left half plane, implying stability, or to the right half plane, for which reversing the sign of $\mathbf{u}$ will again imply stability of the reversed motion.

The three-sphere swimmer: Since a swimmer with two inputs is essentially *underactuated*, and cannot possess steady parallel swimming at any desired orientation and wall-separation, we now consider a swimmer with three actuated spheres, i.e. $m = n = 3$. In this case, the input $\mathbf{u}_e$ resulting in steady parallel swimming at $\mathbf{q}'_e = (y_e, \theta_e)$ is obtained by inverting $\mathbf{G}(\mathbf{q}')$ as

$$\mathbf{u}_e = \mathbf{G}(\mathbf{q}'_e)^{-1}(1\ 0\ 0)^T. \quad (7)$$

In the example of Fig. 1(c), the spheres are arranged in an equilateral triangle with edge length $d = 5$. Fixing $y_e = 7$ and expressing $\mathbf{u}_e$ as a function of θ_e according to (7), we numerically computed the eigenvalues of the associated linearization matrix $\mathbf{A}$. The real part of $\lambda_{1,2}$ as a function of θ_e is shown in Fig. 5(a). The results, which are 120°-periodic due to the symmetry of the triangle, show regions of orientations θ_e for which parallel swimming is stable. Not surprisingly, the transition from stable to unstable swimming occurs at $\theta_e = -30°, 30°$, which correspond to orientations at which the swimmer possesses *mirror symmetry about the line perpendicular to the wall*. Moreover, when θ_e is regarded as a parameter of the dynamical system $\dot{\mathbf{q}}' = \mathbf{G}'(\mathbf{q}')\mathbf{u}(\theta_e)$, the values $\theta_e = -30°, 30°$, associated with an imaginary pair of eigenvalues, correspond to *Hopf bifurcation* with respect to θ_e, indicating existence of periodic orbits [20]. This Hopf bifurcation is inherently *degenerate*, due to the reversing symmetry. Indeed, numerical simulation with $\theta_e = 60°$, corresponding to an unstable equilibrium $\mathbf{q}'_e$, reveal the existence of a *stable periodic orbit*, shown

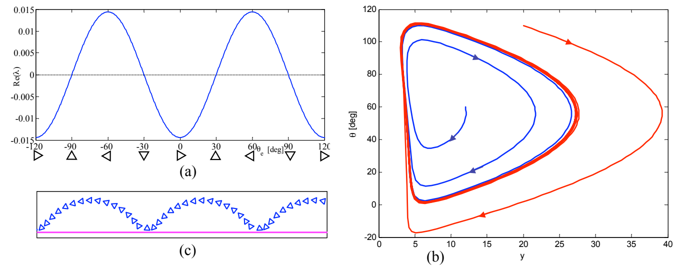

FIG. 5: The three-sphere swimmer- (a): Real part of eigenvalue λ as a function of θ_e (b): Phase plot with a stable periodic orbit for $\theta_e = 60°$. (c): Snapshots of the periodic motion along the wall

in (y, θ) plane in Fig. 5(b). Snapshots of the swimmer's motion along the wall for this (y, θ)-periodic motion are shown in Fig. 5(c). Stable periodic orbits were also obtained numerically in simulations for other values of the parameter θ_e, indicating that whenever the steady parallel swimming is unstable, a stable periodic motion exists.

Finally, it can be shown that the one-parameter family of dynamical systems $\dot{\mathbf{q}}' = \mathbf{G}'(\mathbf{q})\mathbf{u}(\theta_e)$ possesses an additional reversing symmetry with respect to flipping both θ and the parameter θ_e about 30°. For example, trajectories of the system with $\theta_e = 0°$ are obtained from trajectories of the system with $\theta_e = 60°$ by reversing time and flipping θ. Therefore, the system with $\theta_e = 0°$, that has a stable equilibrium $\mathbf{q}'_e$ also has an *unstable periodic orbit*, which is obtained from the stable periodic orbit in Fig. 5(b) by flipping θ about 30° and reversing the time. Moreover, this unstable periodic orbit is precisely the closed curve enclosing the *region of attraction* of the stable equilibrium $\mathbf{q}'_e$ in (y, θ) plane.

Conclusion: We have studied the dynamics and stability of low-*Re* swimming near a wall. We have analyzed the passive stability of swimming parallel to the wall, and highlighted its relation to reversing symmetry of the system. Finally, we have shown the existence of stable periodic motion along the wall. We now briefly sketch some possible directions of future research. The first open problem is a complete characterization of the Hopf bifurcation in this dynamical system by using geometric arguments regarding its reversing symmetries. A second direction is applying nonlinear control techniques for steering articulated micro-swimmers stably in confined environments. Third, accounting for factors such as background flow and effects of inertia will enhance the physical reliability of this model, and will enable investigation of a wider range of phenomena in biological motility. Other possible extension is implementation of numerical methods such as boundary element and multipole expansion in order to simulate more complex swimmers in confined environments of arbitrary shape. Finally, we are currently building an experimental system in order to verify the theoretical results on a macro-scale swimmer prototype in highly viscous silicon oil.

YO was supported by the Fulbright Foundation and the Bikura Scholarship of the ISF.

* izi@cds.caltech.edu

[1] J. Happel and H. Brenner, *Low Reynolds Number Hydrodynamics* (Prentice-Hall, New Jersey, 1965).

[2] S. Kim and S. J. Karrila, *Microhydrodynamics* (Butterworth-Heinemann, Boston, 1991).

[3] E. M. Purcell, Am. J. Phys. **45**, 3 (1977).

[4] A. Shapere and F. Wilczek, J. Fluid Mech. **198**, 557 (1989).

[5] J. E. Avron and O. Raz, New J. Phys. **10**, 063016 (2008).

[6] J. Koiller, R. Montgomery, and K. Ehlers, J. Nonlinear Science **6**, 507 (1996).

[7] J. S. Martin, T. Takahashi, and M. Tucsnak, Quarterly of Applied Mathematics **65**, 405 (2007).

[8] F. Alouges, A. DeSimone, and A. Lefebvre, J. Nonlinear Science **18**, 277 (2008).

[9] D. F. Katz, J. Fluid Mech. **64**, 33 (1974).

[10] M. Ramia, D. L. Tullock, and N. Phan-Thien, Biophysical Journal **65**, 755 (1993).

[11] L. E. Becker, S. A. Koehler, and H. A. Stone, J. Fluid Mech. **490**, 15 (2003).

[12] A. Najafi and R. Golestanian, Phys. Rev. E **69**, 062901062904 (2004).

[13] A. M. Leshansky and O. Kenneth, Phys. Fluids **20**, 063104 (2008).

[14] A. M. Leshansky, O. K. O. Gat, and J. E. Avron, New J. Phys. **9**, 145 (2007).

[15] A. Bernheim-Groswasser, S. Wiesner, R. M. Golsteyn, and M.-F. Carlier, Nature **417**, 308 (2002).

[16] J. W. Swan and J. F. Brady, Phys. Fluids **19**, 113306 (2007).

[17] J. S. W. Lamb and J. A. G. Roberts, Physica D **112**, 1 (1998).

[18] A. P. Berke, L. Turner, H. C. Berg, and E. Lauga, Phys Rev. Lett. **101**, 038102 (2008).

[19] L. J. Fauci and A. McDonald, J. Bull. Math. Biol. **57**, 679 (1995).

[20] J. Guckenheimer and P. Holmes, *Nonlinear Oscillations, Dynamical Systems, and Bifurcations of Vector Fields* (Springer-Verlag, New York, 1983).

[21] S. D. Kelly and R. M. Murray, J. of Robotic Systems **12**, 417 (1995).

[22] J. E. Marsden, *Lectures on Mechanics* (Cambridge Univ. Press, New York, 1992).

[23] R. L. Devaney, Trans. Am. Math. Soc. **218**, 89 (1976).